https://doi.org/10.5194/acp-2021-593
Preprint. Discussion started: 23 July 2021

Atmospheric Chemistry and Physics Discussions

Diverse mixing states of amine-containing single particles in Nanjing, China

Qi En Zhong[1,2], Chunlei Cheng[1,2]*, Zaihua Wang[3*], Lei Li[1,2], Mei Li[1,2], Dafeng Ge[4,5], Lei Wang[4,5], Yuanyuan Li[4,5], Wei Nie[4,5], Xuguang Chi[4,5], Aijun Ding[4,5], Suxia Yang[2,6], Duohong Chen[7], Zhen Zhou[1,2]

[1]Institute of Mass Spectrometry and Atmospheric Environment, Guangdong Provincial Engineering Research Center for on-line source apportionment system of air pollution, Jinan University, Guangzhou 510632, China

[2]Guangdong-Hongkong-Macau Joint Laboratory of Collaborative Innovation for Environmental Quality, Guangzhou 510632, China

[3]Institute of Resources Utilization and Rare Earth Development, Guangdong Academy of Sciences, Guangzhou 510651, China

[4]Joint International Research Laboratory of Atmospheric and Earth System Sciences (JirLATEST), School of Atmospheric Sciences, Nanjing University, Nanjing 210023, China

[5]Collaborative Innovation Center of Climate Change, Jiangsu Province, Nanjing 210023, China

[6]Institute for Environment and Climate Research, Jinan University, Guangzhou 510632, China

[7]State Environmental Protection Key Laboratory of Regional Air Quality Monitoring, Guangdong Environmental Monitoring Center, Guangzhou 510308, China

*Correspondence to: Chunlei Cheng (chengcl@jnu.edu.cn) and Zaihua Wang (zaihuawang@163.com)

Tel: 86-20-85225991, Fax: 86-20-85225991

https://doi.org/10.5194/acp-2021-593
Preprint. Discussion started: 23 July 2021

Atmospheric Chemistry and Physics Discussions

Abstract: The mixing states of particulate amines with different chemical components are of great significance in studying the formation and evolution processes of amine-containing particles. In this work, the mixing states of single particles containing trimethylamine (TMA) and diethylamine (DEA) are investigated in order to study the formation and aging processes of the single particles using a high-performance single-particle aerosol mass spectrometer located in Nanjing, China, in September 2019. TMA- and DEA-containing particles accounted for 22.8% and 5.5% of the total detected single particles, respectively. The particle count and abundance of the TMA-containing particles in total particles notably increased with enhancement of ambient relative humidity (RH), while the DEA-containing particles showed no increase under a high RH. This result suggested the important role of RH in the formation of particulate TMA. Significant enrichments of secondary organic species, including $^{43}C_2H_3O^+$, $^{26}CN^-$, $^{42}CNO^-$, $^{73}C_3H_5O_2^-$, and $^{89}HC_2O_4^-$, were found in DEA-containing particles, indicating that DEA-containing particles were closely associated with the aging of secondary organics. The particle count and abundance of DEA-containing particles showed a prominent increase during the nighttime, but a sharp decrease during the afternoon. Furthermore, the differential mass spectra of the DEA-containing particles showed a much higher abundance of nitrate during the nighttime than during the daytime. In addition, the number fraction of organic nitrogen species in the DEA-containing particles and ambient NOx both showed consistent increasing trends, similar to the accumulation of DEA-containing particles during the nighttime. This suggested that the nighttime production of particulate DEA might be associated with reactions of gaseous DEA with HNO_3 and/or particulate nitrate. Higher abundances of oxalate and glyoxylate were found in DEA-containing particles during the strong photochemistry period when the abundance of DEA-containing particles decreased to the lowest of the total particles. This result suggested a substantial impact of photochemistry on the aging process of DEA-containing particles. Further, greater than 80% of TMA- and DEA-containing particles internally mixed with nitrate, while the abundance of sulfate was higher in the DEA-containing particles (79.3%) than in the TMA-containing particles (55.3%).

https://doi.org/10.5194/acp-2021-593
Preprint. Discussion started: 23 July 2021


Atmospheric Chemistry and Physics Discussions

In addition, a lesser amount of ammonium was found in the DEA-containing particles (13.2%) compared with the TMA-containing particles (35%). These observations suggested that particulate DEA existed both as nitrate and sulfate aminium salts, while the particulate TMA primarily presented as nitrate aminium salt. Overall, the different mixing states of the TMA- and DEA-containing particles suggested their different formation processes and various influencing factors, which are difficult to be investigated using bulk analysis. These results provide insights into the discriminated fates of organics during the evolution process in aerosols, which provides a better illustration of the behavior of secondary organic aerosols.

Keywords: Amines; Single particle; Mixing state; Nighttime chemistry; Aminium salts.

1 Introduction

Amines are ubiquitous organic components in aerosols and have a wide range of sources, including animal husbandry, industrial emissions, vehicle exhaust, biomass burning, vegetation emissions, and ocean emissions (Ge et al., 2011a; Facchini et al., 2008; Youn et al., 2015). Due to being highly water-soluble and having strong alkaline properties, amines play an important role in new particle formation and substantially contribute to the secondary organic aerosol (SOA) mass (Zhao et al., 2011; Tao et al., 2016). The formation processes of particulate amines are commonly associated with the gas-to-particle partitioning of gaseous amines and acid-base reactions in the particles (Ge et al., 2011b; Pratt et al., 2009). Therefore, ambient relative humidity (RH) (Rehbein et al., 2011; Zhang et al., 2012), temperature (T) (Huang et al., 2012), particle acidity (Pratt et al., 2009; Rehbein et al., 2011), amine-ammonium exchange (Chan and Chan, 2013; Chu and Chan, 2017; Qiu et al., 2011), and oxidants (Tang et al., 2013; Price et al., 2016) all influence the formation of particulate amines.

Many field observations have been used to investigate the influence of RH on the formation of amines. A high RH is beneficial for the formation of amines in most

https://doi.org/10.5194/acp-2021-593
Preprint. Discussion started: 23 July 2021


Atmospheric Chemistry and Physics Discussions

cases. Zhang et al. (2012) observed a sharp increase in trimethylamine (TMA) during fog events with high RH. Zhou et al. (2019) found that the concentrations of low molecular weight (LMW) amines increased significantly under high RH conditions (> 90%). According to the seasonal distributions of amines during the summer and winter, low T was found to be favorable for the partitioning of gaseous amines into particles. Huang et al. (2012) found that the number fraction (N_f) of amine-containing particles during winter was four times higher than that during summer.

Gaseous amines can react with sulfuric acid, nitric acid, and organic acids to form aminium salts, which underscores the important roles of sulfate and nitrate information of particulate amines (Murphy et al., 2007; Berndt et al., 2010). Berndt et al. (2010) and Wang et al. (2010) found that the formation of aminium salts via a neutralization reaction can affect the growth of particles and the generation of SOAs, which was even stronger than that of NH_3. Although amine concentrations are generally lower than ammonia and ammonium, the amine-ammonium exchange still contributes to particulate amine formation due to the stronger alkalinity of amines compared to ammonium (Ge et al., 2011a; Sorooshian et al., 2008). Chan et al. (2013) found that the exchange reactions between ammonia and amines showed different reaction rates and product ratios with changes in the aerosol phase state. Qiu et al. (2011) also found that amines can exchange with ammonium to release ammonia. The particulate amines produced from the above pathways and reactions constitute a substantial proportion of the SOAs that impact the physical and chemical properties of fine particles. In addition to the direct contribution of the SOA mass, the oxidation of amines by OH radicals, NO_3 radicals, and O_3 is also a substantial source of SOA production. Different amines (NO_3 radicals, OH radicals, and ozone) exhibit inconsistent behaviors under the same oxidation environments (Murphy et al., 2007; Price et al., 2014; Silva et al., 2008). In chamber studies, the oxidation of TMA and diethylamine (DEA) by OH vs. NO_3 radicals resulted in different SOA yields, with differences greater than one order of magnitude (Tang et al., 2013). Furthermore, even the same amine showed completely different SOA yields due to OH and NO_3 radical oxidation. Also, the same amine showed distinct trends under the different

https://doi.org/10.5194/acp-2021-593
Preprint. Discussion started: 23 July 2021


Atmospheric Chemistry and Physics Discussions

120 temperature changing trends. The formation and oxidation processes of particulate
121 amines are not well understood, and these processes require additional comprehensive
122 field observational studies in order to be elucidated.

123 Most of the field observations did not distinguish between the different behaviors
124 of each type of amine molecule under the same ambient influencing factors. Actually,
125 due to the different mixing states of amines with other chemical components, the
126 amine molecules typically exhibited different behaviors in terms of being oxidized by
127 OH radicals, forming aminium salts, and altering the hygroscopicity of the particles
128 (Healy et al., 2015; Cheng et al., 2018; Chu et al., 2015; Price et al., 2016). Therefore,
129 the formation processes of the different amines are important to reveal the evolution
130 process of organic aerosols (OAs), and these processes are of great significance to
131 comprehensively understand the influencing factors of OA production.

132 Recently, real-time identification of single particles has become an effective
133 technique to measure the mixing states of diverse amine-containing single particles,
134 providing a feasible approach to investigate the formation processes of different
135 particulate amines (Chen et al., 2019; Lian et al., 2020; Cheng et al., 2018). Chen et al.
136 (2019) found that high RH was favorable for the uptake of DEA, leading to a
137 DEA-rich substance in the particle phase both during winter and summer. However,
138 Cheng et al. (2018) and Lian et al. (2020) found that RH was not strongly correlated
139 with the formation of amine-containing particles during winter and summer. Pratt et al.
140 (2009) reported that more acidic particles during summer were favorable for the
141 formation of aminium salts compared with the particles present during autumn,
142 indicating that the particle acidity affected the gas to particle partitioning of amines.
143 Rehbein et al. (2011) found more TMA entered the particles as the amount of acidic
144 particles increased. Based on these studies, although the influences of ambient RH
145 and particle acidity on the specific type amines formed have been reported, yet
146 comparative studies between different amines under the same atmospheric
147 environment using field observation are lacking.

148 In the present study, the mixing states of TMA- and DEA-containing single
149 particles are investigated during autumn using a high performance single particle

https://doi.org/10.5194/acp-2021-593
Preprint. Discussion started: 23 July 2021


Atmospheric Chemistry and Physics Discussions

aerosol mass spectrometer (HP-SPAMS) located in Nanjing, China. Two types of amine-containing particles exhibited different mixing states with secondarily produced OA species. The influences of ambient RH, T, and particle acidity on the mixing states of the two amine-containing particles are evaluated. In addition, the potential heterogeneous formation of DEA during the nighttime is also discussed. The results revealed the distinct chemical behaviors of TMA- and DEA-containing particles and implied the potential role of DEA as an indicator of the aging process of OA.

2 Experimental methods

2.1 Sampling site

Ambient single particles were sampled using the HP-SPAMS from September 2–16, 2019, in Nanjing, China. The sampling site is constantly influenced by anthropogenic emissions due to its downwind location from urban areas (Figure S1) (Ding et al., 2013a; Ding et al., 2013b; Ding et al., 2016). The instrument was set up on top of a small hill (40 m above the ground) on the Nanjing University campus. The ambient single particles were introduced into the HP-SPAMS through a copper tube.

2.2 Instrumentation of the HP-SPAMS

In this work HP-SPAMS (Hexin Analytical Instrument Co., Ltd., China) was used to detect single particles. The design and principles of SPAMS had previously been described in detail (Li et al., 2011). In short, particles are introduced into the aerodynamic lens through a critical orifice at a specific flow rate. Individual particles are focused and accelerated to specific velocities, which are detected by two continuous diode Nd:YAG laser beams (532 nm) and then ionized using a pulsed Nd:YAG laser (266 nm). Finally, the z-shaped bipolar time of the flight mass spectrometer is used to detect the generated ions. The improvements and modifications from the SPAMS to the HP-SPAMS are comparatively presented below. The improvement in the SPAMS primarily includes three portions: the application of a concentration device, a delay extraction technology, and a multichannel acquisition technology (Chen et al., 2020; Li et al., 2018). First, the addition of the concentrator

https://doi.org/10.5194/acp-2021-593
Preprint. Discussion started: 23 July 2021


Atmospheric Chemistry and Physics Discussions

increases the injection flow rate by six times, which allows for improved separation of gas and particles. Second, since the positions of the ionized ions scatter instead of being completely linear in the same direction, delayed extraction technology is used in SPAMS to replace the constant electrical field extraction technique. This delays the ions in order to obtain sufficient potential energy in the appropriate time under a pulsed electric field and captures faster ions to improve the resolutions of positive and negative ions. The mass resolutions of the positive (> 1000 at maximum half width) and negative (> 2000 at maximum half width) ion spectra are then significantly improved. Third, the multichannel acquisition technology is used to divide the signal into two channels, detecting the high and low intensity signals simultaneously without signal loss. This new acquisition technology enables a detectable dynamic signal from 5–20000 mV, which is approximately 40 times higher than that of SPAMS.

2.3 Data analysis

The size and chemical compositions of single particles obtained using the HP-SPAMS were analyzed using the Computational Continuation Core (COCO) toolkit in MATLAB software. According to previous studies that have utilized aerosol time-of-flight mass spectrometer (ATOFMS) and SPAMS, the amine-containing particles were identified by querying $^{59}(CH_3)_3N^+$, $^{74}(C_2H_5)_2NH_2^+$, $^{86}(C_2H_5)_2NCH_2^+$, $^{101}(C_2H_5)_3N^+$, $^{102}(C_3H_7)_2NH_2^+$, and $^{143}(C_3H_7)_3N^+$ (Healy et al., 2015; Angelino et al., 2001; Cheng et al., 2018; Zhang et al., 2012). In this work, the marker ions of $^{59}(CH_3)_3N^+$, $^{74}(C_2H_5)_2NH_2^+$, and $^{86}(C_2H_5)_2NCH_2^+$ were detected as the abundant species, and their particle counts and ratios in the total detected single particles are shown in Table 1. Single particles containing $^{86}(C_2H_5)_2NCH_2^+$ only accounted for 3.7% of total particles, which was primarily due to occasional increases on September 5 (Figure S2), possibly due to the outburst of special emissions, such as combustion and industry. Thus, in this work, particles containing $^{59}(CH_3)_3N^+$ and $^{74}(C_2H_5)_2NH_2^+$ were selected to discuss the mixing states and formation processes of the particulate amines. The maker ions of $^{62}NO_3^-$, $^{97}HSO_4^-$, and $^{18}NH_4^+$ were used to identify the nitrate, sulfate, and ammonium in the amine-containing particles (Zhang et al., 2012). Based on field and chamber studies using SPAMS and ATOFMS, the $^{43}C_2H_3O^+$ ion was

https://doi.org/10.5194/acp-2021-593
Preprint. Discussion started: 23 July 2021


Atmospheric Chemistry and Physics Discussions

identified as the representative oxygen-containing organic (Healy et al., 2015; Pratt et al., 2009). The particles containing $^{26}CN^-$ and $^{42}CNO^-$ were considered to be representative of the organic nitrogen-containing particles (Pratt et al., 2011). In addition, the $^{73}C_3H_5O_2^-$ and $^{89}HC_2O_4^-$ ions were designated as glyoxylate and oxalate markers, respectively (Cheng et al., 2017; Zhang et al., 2020).

3 Results and discussion

3.1 Characteristics of amine-containing particles

In this work, the amine-containing particles accounted for 32.1% of total detected single particles, which was higher than in previously reported results for the Pearl River Delta (PRD) region (9.4%–11.1%) and Chongqing (8.3%–12.7%), China. The TMA-containing particles showed a much higher abundance in the total particles (22.8%) than the DEA-containing particles (5.5%) (Table 1), which could have been due to their differential emissions and atmospheric processing (Cheng et al., 2018; Chen et al., 2019; Liu et al., 2020; Ge et al., 2011a). Temporal variations in meteorological parameters, $PM_{2.5}$ concentration, and the count of amine-containing particles are shown in Figure 1. Although the TMA- and DEA-containing particles exhibited similar temporal trends at a lower particle count, their increasing peaks appeared at different periods, suggesting that the reasons for their increase in the particle count were different. Generally, peaks in the DEA-containing particles frequently appeared during the nighttime, which was possibly due to their enhanced source emissions and/or favorable nighttime production (Tang et al., 2013). The ambient RH was relatively high during the entire sampling period ($74 \pm 14\%$), especially from September 5–7, when the count of TMA-containing particles sharply increased. However, no obvious enhancement in DEA-containing particles count was found, which suggested other influencing factors on their formation process in addition to the ambient RH.

Additionally, the periods of high concentration of the amine-containing particles were not consistent with the increase in $PM_{2.5}$ concentration, which could have been due to the integrated effects of the emission sources and the secondary formation

https://doi.org/10.5194/acp-2021-593
Preprint. Discussion started: 23 July 2021


Atmospheric Chemistry and Physics Discussions

processes. The backward trajectories of the air masses (48 h, 500 m) associated with the spatial distributions of the two amine-containing particles during the entire sampling period are presented in Figure 2. More than 70% of the air masses (Clusters 1 and 4) were from east of the sampling site, which were both connected with anthropogenic emissions in the Yangtze River Delta (YRD) and marine sources in the East China Sea. TMA-containing particles were primarily from the air masses of Cluster 1 and Cluster 4, while the DEA-containing particles were associated with the air masses of Cluster 3 and Cluster 4, which underwent long-range transport. These results suggested potential different emission sources and atmospheric formation processes of TMA- and DEA-containing particles, which was further investigated by examining their mixing states.

Diurnal variations of TMA- and DEA-containing particles are shown in Figure 3. The particle count of TMA-containing particles and their abundance in the total particles exhibited identical variation patterns. These patterns exhibited significant increases in the morning, possibly associated with direct emissions from vehicle exhaust (Chen et al., 2019; Cheng et al., 2018). The DEA-containing particles showed a completely different diurnal pattern compared with the TMA-containing particles. DEA-containing particles increased during nighttime, but sharply decreased during the afternoon, when the photochemistry was the most active. The nighttime increase could have been due to the high ambient RH and/or enhanced heterogeneous reactions (Zhou et al., 2019; Huang et al., 2012; Zhang et al., 2019). However, since the increase in the DEA-containing particles was not prominent under high RH (Figure 1), enhanced heterogeneous production of particulate DEA could be a more reasonable explanation. The decrease in the DEA-containing particles during the afternoon could have been associated with the photodegradation of DEA and/or repartitioning of particulate DEA under high temperatures during the day (Murphy et al., 2007; Ge et al., 2011b; Pitts et al., 1978). In order to investigate the impact of ambient RH on the formation process of amine-containing particles, the particle counts of amine particles and the relative peak areas (RPAs) of amines in the particles with an increase in the ambient RH are presented in Figure 4. The particle count of TMA-containing particles

https://doi.org/10.5194/acp-2021-593
Preprint. Discussion started: 23 July 2021


Atmospheric Chemistry and Physics Discussions

and the RPA of the TMA showed remarkable increasing trends with an enhancement in RH during the entire sampling period. This result suggested a significant role of RH in the formation of particulate TMA. This was consistent with a field study conducted in Guangzhou, China, which also found an instant increase in TMA-containing particles after the occurrence of fog events (Zhang et al., 2012). In contrast, the particle count of DEA-containing particles only exhibited increased RH range between 70–80% and decreased with the continuous increase in the RH. Additionally, the RPA of the DEA showed little change with an increase in the RH, which suggested the minor influence of a change in RH on the formation of particulate DEA. The different responses of TMA and DEA with RH changes signified their different formation processes in the particles.

3.2 Different mixing states of amine-containing particles

It is important to understand the chemical compositions of amine-containing particles in order to understand their mixing states and track their formation processes. Hence, the positive and negative mass spectra of the amine-containing particles are shown in Figure 5. Generally, TMA- and DEA-containing particles both contained amine marker ions, as well as organic fragments such as $^{27}C_2H_3^+$, $^{37}C_3H^+$, $^{43}C_2H_3O^+$, $^{51}C_4H_3^+$, and $^{61}C_5H^+$ in the positive mass spectra. In addition, their negative mass spectra were both characterized by nitrate, sulfate, and nitric acid ($^{125}H(NO_3)_2^-$). However, DEA-containing particles contained many more organic fragments and a higher abundance of hydrocarbon clusters than the TMA-containing particles. In the positive mass spectra, the abundance of the hydrocarbon fragments with an m/z below 60 was 2–3 times higher in DEA-containing particles than that in TMA-containing particles. In addition, hydrocarbon fragments with an m/z above 60 were barely detectable in TMA-containing particles, while abundant hydrocarbon fragments with an m/z ranging from 60–150 were observed in DEA-containing particles. Furthermore, the DEA-containing particles also contained abundant secondary organic marker ions, including organic nitrogen ($^{26}CN^-$ and $^{42}CNO^-$), acetate ($^{59}C_2H_3O_2^-$), glyoxylate ($^{73}C_3H_5O_2^-$), and oxalate ($^{89}HC_2O_4^-$) in the negative mass spectra, and these were not found in the TMA-containing particles. This was in accordance with the linear

https://doi.org/10.5194/acp-2021-593
Preprint. Discussion started: 23 July 2021


Atmospheric Chemistry and Physics Discussions

298 regressions between these secondary organic ions containing particles with two
299 amine-containing particles (Table 2), which showed no correlations in the
300 TMA-containing particles ($r^2 < 0.1$), but good correlations in the DEA-containing
301 particles ($r^2 > 0.57$). The differential mass spectral features in the distributions of
302 organics in the two amine-containing particles (Figure 6) suggested that more
303 secondary organics accumulated in DEA-containing particles than in TMA-containing
304 particles. This result also implied that multiple factors influenced the mixing state of
305 DEA-containing particles in addition to ambient RH.

306 In order to further characterize the mixing states of DEA-containing particles
307 with secondary organic ions, temporal variations and diurnal patterns of secondary
308 organic ions in the DEA-containing particles are presented in Figure 7. As the
309 oxidation products of various organics, the abundances of glyoxylate and oxalate
310 commonly increased between 12:00 and 18:00 (Figure 7), when the photochemistry
311 was most active during the daytime. This result suggested the deep photochemical
312 aging state of DEA-containing particles. This might explain the decrease in the
313 particle counts of DEA-containing particles (Figure 3), which was partially associated
314 with the photo-degradation of particulate DEA. Pitts et al. (1978) reported that under
315 sunlight particulate DEA decomposed to acetamide, while DEA in the gas phase was
316 oxidized to acetaldehyde, PAN, amide, and imine. Gaseous DEA can be oxidized into
317 carbonyl compounds and other amines by ozone and OH radicals that primarily
318 include acetaldehyde and N-ethylethanimine (Tuazon et al., 2011; Tong et al., 2020).
319 The organic nitrogen markers of $^{26}CN^-$ and $^{42}CNO^-$ showed different temporal trends
320 with glyoxylate and oxalate. Although the abundances of organic nitrogen markers
321 also increased after 12:00 like oxalate, the markers still maintained high abundances
322 during the nighttime, when glyoxylate and oxalate sharply decreased. This result
323 suggested that the aging process of organics during the nighttime was slower than that
324 during the afternoon in the DEA-containing particles. Thus, the increase of
325 DEA-containing particles (Figure 3) could have been due to the enhanced production
326 of particulate DEA during the nighttime. In addition, the differential mass spectra of
327 DEA-containing particles (Figure 8) between the nighttime (22:00–02:00) and

https://doi.org/10.5194/acp-2021-593
Preprint. Discussion started: 23 July 2021


Atmospheric Chemistry and Physics Discussions

daytime (14:00–18:00) showed a significant enrichment of nitrate during the nighttime. This result suggested that nighttime production of particulate DEA was associated with gaseous HNO_3 and/or particulate nitrate (Price et al., 2016).

Temporal variations in NOx and the N_f of the DEA-containing particles in the total detected particles are presented in Figure 9. They showed similar increasing patterns during the nighttime, and a high abundance of nitrate in the DEA-containing particles was also observed. This result suggested the important role of nitrate in the formation of particulate DEA. The particulate DEA during the nighttime could have been produced from the reaction of gaseous DEA with HNO_3 during the gas phase (R1) followed by the gas to particle partitioning (R2) and/or the direct heterogeneous formation pathway (R3) (Price et al., 2016; Nielsen et al., 2012). The high ambient concentration of NOx is favorable for the production of NO_3 radicals and the heterogeneous production of nitrate, which might explain the distinct enhancement of the DEA-containing particles. However, the same formation pathways were also applied to TMA, yet there was no significant increase in the N_f of the TMA-containing particles in the total particles (Figure 3). This could have been due to the different particle/gas dissociation constant (K_p) for DEA ⊣HNO_3 and TMA ⊣HNO_3, which was several orders of magnitude lower than that for DEA ⊣HNO_3 (7.01E-09) compared with TMA ⊣HNO_3 (1.65E-06) at 25 ℃ (Price et al., 2016; Ge et al., 2011b). During the entire sampling period, the ambient temperature during the nighttime was approximately 24 ℃. Thus, the produced DEA ⊣HNO_3 tended to stay in the particles, while a portion of the TMA ⊣HNO_3 repartitioned back into the gas phase. This resulted in an insignificant increase in the TMA-containing particles. Further studies should consider the influence of the different volatilities of DEA ⊣HNO_3 and TMA ⊣HNO_3 on the formation of particulate amines in chamber experiments due to the lack of quantitative results in this study.

$$(CH_3CH_2)_2NH_{(g)} + HNO_{3(g)} \rightarrow (CH_3CH_2)_2N\ \dashv HNO_{3(g)}. \quad \text{(R1)}$$

$$(CH_3CH_2)_2N\ \dashv HNO_{3(g)} \leftrightarrow (CH_3CH_2)_2N\ \dashv HNO_{3(s)}. \quad \text{(R2)}$$

$$(CH_3CH_2)_2NH_{(g)} + NO_3^-{}_{(s)} \rightarrow (CH_3CH_2)_2N\ \dashv HNO_{3(s)}. \quad \text{(R3)}$$

3.3 Formation of aminium salts

https://doi.org/10.5194/acp-2021-593
Preprint. Discussion started: 23 July 2021


Atmospheric Chemistry and Physics Discussions

To study the acid-base reactions of TMA and DEA with sulfate and nitrate, the N_fs of nitrate-, sulfate-, and ammonium-containing particles in total detected particles and amine-containing particles are shown in Table 3. More than 80% of TMA- and DEA-containing particles internally mixed with nitrate, which was higher than the N_f of nitrate in the total particles (72%). Interestingly, the N_f of sulfate in DEA-containing particles (79.3%) was much higher than that in TMA-containing particles (55.3%) and in the total particles (60.1%). This was similar to a study performed by Lian et al. (2020) that found a stronger correlation between $^{86}(C_2H_5)_2NCH_2^+$ with sulfate than that between TMA and sulfate. In addition, in this work, robust linear correlations ($r^2 > 0.9$) between nitrate-containing particles and amine particles were both observed in TMA- and DEA-containing particles (Table 2). However, a weak linear correlation ($r^2 = 0.32$) was found between the sulfate-containing particles and the TMA-containing particles, while a better linear correlation ($r^2 = 0.86$) was observed in the DEA-containing particles. According to reported studies, the vapor pressure of diethylaminium sulfate (DEAS) ($0.2*10^{-12}$–$12.8*10^{-12}$ Pa) was three orders of magnitude lower than that of trimethylaminium sulfate (TMAS) ($0.6*10^{-9}$–$1.8*10^{-9}$ Pa) at 298 k. In addition, the enthalpy of evaporation was higher than that of TMAS (DEAS: 168 ± 5 kJ mol^{-1}; TMAS: 114 ± 2 kJ mol^{-1}) (Lavi et al., 2013). Therefore, the thermo-stability of DEAS was stronger than TMAS (Qiu and Zhang, 2012), which led to the higher N_f of sulfate in the DEA-containing particles than in the TMA-containing particles.

The N_f of ammonium in DEA-containing particles (13.2%) was lower than in TMA-containing particles (35%) and total particles (19.4%). The low abundance of NH_4^+ in DMA-containing particles had been observed in our previous studies in the PRD region (Cheng et al., 2018), which was partially attributed to the ammonium-amine exchange reactions in the particles. The related laboratory experiments primarily involved the preferential uptake of LMW amines in the H_2SO_4 particles (Sauerwein and Chan, 2017; Chan and Chan, 2013; Chu and Chan, 2017). In this work, the distinct low N_f of NH_4^+ in the DEA particles suggested the possible displacement of NH_4^+ by DEA. Moreover, the higher abundance of sulfate in DEA

https://doi.org/10.5194/acp-2021-593
Preprint. Discussion started: 23 July 2021


Atmospheric Chemistry and Physics Discussions

particles than in TMA particles was more favorable for the occurrence of ammonium-amine exchange reactions in DEA particles. This disparity could imply differential roles of DEA and TMA in the new particle formation process (Wang et al., 2010; Yin et al., 2011; Zhao et al., 2011).

The temporal trends of the N_fs of nitrate-, sulfate-, and ammonium-containing particles in TMA and DEA particles are shown in Figure 10. The N_f of nitrate-containing amine particles exhibited similar variation patterns with each type of amine particle, while the N_f of sulfate-containing amine particles only showed a similar variation pattern with DEA-containing particles. Although aminium nitrate and sulfate salts were both produced in TMA- and DEA-containing particles, the different temporal trends of sulfate and nitrate in the two amine particles suggested that both sulfate and nitrate DEA salts existed in the DEA-containing particles, while nitrate TMA salt dominated in TMA-containing particles (Cheng et al., 2018; Pratt et al., 2009). This difference in the form of aminium salts could signify the potential different influences in the hygroscopic property of secondarily processed particles internally mixing with different amines (Rovelli et al., 2017; Clegg et al., 2013; Lavi et al., 2013). The relative acidity ratio (Ra), defined as the ratio of the sum of the sulfate and nitrate peak areas to the ammonium peak area, has been proposed in field studies that use single particle mass spectrometry to roughly estimate particle acidity (Huang et al., 2013; Cheng et al., 2018). In this work, temporal variations in Ra in TMA-containing particles (Ra_1) and DEA-containing particles (Ra_2) are shown in Figure 11. The average Ra_1 was 6.3 ± 1.8 in TMA-containing particles, and Ra_2 was 36.1 ± 21.8 in DEA-containing particles. This result could suggest a more acidic nature of DEA particles than TMA particles. However, after including the peak area of amines (TMA/DEA) in the calculation of Ra, the new Ra′ was reduced to 2.1 ± 0.5 in the TMA-containing particles and 6.5 ± 1.2 in the DEA-containing particles. The gap of Ra between the two amine particles significantly decreased after including amines in the calculation. The larger reduction ratio of Ra′ in DEA-containing particles than in TMA-containing particles suggested the effective buffering effect of amines under the absence of ammonium in the particles.

https://doi.org/10.5194/acp-2021-593
Preprint. Discussion started: 23 July 2021


Atmospheric Chemistry and Physics Discussions

3.4 Implications of the diverse mixing states of amines particles

The mixing states and formation processes of the two amine-containing particles were investigated under the same atmospheric environment, and their different atmospheric behaviors against the same influencing factors suggested their differential contributions to SOA mass. The prominent impact of ambient RH on the formation of particulate TMA suggested a significant role for gas-particle partitioning process to the high water-soluble species in the SOA. However, the slight influence of RH on the formation of the particulate DEA implied the inconsistent role of high RH on the same group of water-soluble organic molecules. In addition, the distinct distribution patterns of secondary organic species in two amine-containing particles also signified that the mixing states of the OA are important to explore their formation processes. Furthermore, the heterogeneous processing of the DEA-containing particles during the nighttime and the photochemical degradation of the DEA during the daytime both generated more fractions of nitrogen- and oxygen-containing species in the particles than in the TMA-containing particles. This result suggested different roles of particulate TMA and DEA in the evolution of hygroscopicity and aging state of the SOA. In summary, understanding mixing states and formation processes of different amines in single particles is of great significance to reveal the unique response of each type of amine to the same atmospheric environment. Single-particle analysis provided insights into the mixing states of specific organic species to further understand the formation process of the SOA.

4 Summary and conclusions

TMA- and DEA-containing single particles were collected and analyzed on September 2019 using HP-SPAMS in Nanjing, China, and accounted for 22.8% and 5.5% of total detected particles, respectively. The mixing states and formation processes of TMA- and DEA-containing particles were studied. With increased RH, the counts of particulate TMA and the RPA of the TMA displayed an obvious upward trend, while the particle count of the particulate DEA slightly increased when the RH was 70–80%. In addition, the RPA of the DEA showed no difference in reaction to

https://doi.org/10.5194/acp-2021-593
Preprint. Discussion started: 23 July 2021


Atmospheric Chemistry and Physics Discussions

RH change during the entire sampling period. This suggested a differential role for ambient RH during the formation processes of particulate TMA and DEA. The possible formation processes were further evaluated by analyzing the mixing states of the amine-containing particles. The mass spectra of the amine-containing particles showed that the secondary organic species were enriched in the DEA-containing particles. The differential distributions of the secondary ions effectively explained the sharp increase in DEA-containing particles during the nighttime, which could have been due to the heterogeneous reactions of gaseous DEA with HNO_3 and/or nitrate particles. The prominent decrease in the DEA-containing particles during the afternoon was attributed to photo-degradation of particulate DEA. Due to the differences in the thermodynamic properties, the N_f of sulfate in the particulate DEA was higher than that in the particulate TMA. The amine-ammonium exchange reaction resulted in particulate DEA containing less NH_4^+. In addition, the particulate DEA was abundant in sulfate, which was more favorable for the exchange of amine and ammonium. The higher relative acidity ratio in DEA-containing particles relative to TMA-containing particles could suggest that DEA particles are more acidic. After including the peak area of amines (TMA/DEA) in the calculation, the larger reduction ratio of the Ra′ in DEA-containing particles than in TMA-containing particles suggested the effective buffering effect of amines under the absence of ammonium in the particles. These results revealed the distinct mixing states and chemical behaviors of TMA- and DEA-containing single particles and could imply a potential role for DEA as an indicator of the OA aging process.

Data availability

The observational data, including HP-SPAMS and the meteorological parameters, obtained in this study are available from the corresponding authors upon request (chengcl@jnu.edu.cn).

Author contribution

https://doi.org/10.5194/acp-2021-593
Preprint. Discussion started: 23 July 2021

Atmospheric Chemistry and Physics Discussions

476 **Qi En Zhong, Chunlei Cheng, Zaihua Wang:** methodology, writing original
477 draft. **Dafeng Ge, Lei Wang, Yuanyuan Li, Wei Nie, Xuguang Chi, Aijun Ding:**
478 methodology, sampling. **Lei Li, Mei Li, Suxia Yang, Duohong Chen, Zhen Zhou:**
479 providing discussions and helping to revise original draft.
480
481 **Competing interests**
482 I declare that I or my co-authors have competing interests as follows: Aijun Ding
483 is editor of ACP.
484
485 **Acknowledgements**: This work was financially supported by the National Key
486 Research and Development Program of China (Grant No. 2018 YFE0106900), the
487 National Natural Science Foundation of China (Grant Nos. 41805093, 41827804 and
488 41875175), the NSFC of Guangdong Province (Grant No. 2021A1515011206), the
489 Guangzhou Economic and Technological Development District International Science
490 and Technology Cooperation Project (Grant No. 2018GH08), the National Research
491 Program for Key Issues in Air Pollution Control (Grant No. DQGG0107), the Pearl
492 River Nova Program of Guangzhou (No. 201806010064), and GDAS' Project of
493 Science and Technology Development (2021GDASYL-20210103058).
494
495 ## References
496 Angelino, S., Suess, D. T., and Prather, K. A.: Formation of aerosol particles from
497 reactions of secondary and tertiary alkylamines: characterization by aerosol
498 time-of-flight mass spectrometry, Environmental science & technology, 35,
499 3130-3138, 10.1021/es0015444, 2001.
500 Berndt, T., Stratmann, F., Sipilä, M., Vanhanen, J., Petäjä, T., Mikkilä, J., Grüner, A.,
501 Spindler, G., Lee Mauldin Iii, R., Curtius, J., Kulmala, M., and Heintzenberg, J.:
502 Laboratory study on new particle formation from the reaction OH +SO2:
503 influence of experimental conditions, H2O vapour, NH3 and the amine
504 tert-butylamine on the overall process, Atmospheric Chemistry and Physics, 10,
505 7101-7116, 10.5194/acp-10-7101-2010, 2010.

https://doi.org/10.5194/acp-2021-593
Preprint. Discussion started: 23 July 2021

506 Chan, L. P. and Chan, C. K.: Role of the aerosol phase state in ammonia/amines
507 exchange reactions, Environmental science & technology, 47, 5755-5762,
508 10.1021/es4004685, 2013.
509 Chen, Y., Kozlovskiy, V., Du, X., Lv, J., Nikiforov, S., Yu, J., Kolosov, A., Gao, W.,
510 Zhou, Z., Huang, Z., and Li, L.: Increase of the particle hit rate in a laser
511 single-particle mass spectrometer by pulse delayed extraction technology,
512 Atmospheric Measurement Techniques, 13, 941-949, 10.5194/amt-13-941-2020,
513 2020.
514 Chen, Y., Tian, M., Huang, R.-J., Shi, G., Wang, H., Peng, C., Cao, J., Wang, Q.,
515 Zhang, S., Guo, D., Zhang, L., and Yang, F.: Characterization of urban
516 amine-containing particles in southwestern China: seasonal variation, source, and
517 processing, Atmospheric Chemistry and Physics, 19, 3245-3255,
518 10.5194/acp-19-3245-2019, 2019.
519 Cheng, C., Huang, Z., Chan, C. K., Chu, Y., Li, M., Zhang, T., Ou, Y., Chen, D.,
520 Cheng, P., Li, L., Gao, W., Huang, Z., Huang, B., Fu, Z., and Zhou, Z.:
521 Characteristics and mixing state of amine-containing particles at a rural site in
522 the Pearl River Delta, China, Atmospheric Chemistry and Physics, 18,
523 9147-9159, 10.5194/acp-18-9147-2018, 2018.
524 Cheng, C., Li, M., Chan, C. K., Tong, H., Chen, C., Chen, D., Wu, D., Li, L., Wu, C.,
525 Cheng, P., Gao, W., Huang, Z., Li, X., Zhang, Z., Fu, Z., Bi, Y., and Zhou, Z.:
526 Mixing state of oxalic acid containing particles in the rural area of Pearl River
527 Delta, China: implications for the formation mechanism of oxalic acid,
528 Atmospheric Chemistry and Physics, 17, 9519-9533, 10.5194/acp-17-9519-2017,
529 2017.
530 Chu, Y. and Chan, C. K.: Reactive Uptake of Dimethylamine by Ammonium Sulfate
531 and Ammonium Sulfate-Sucrose Mixed Particles, The journal of physical
532 chemistry. A, 121, 206-215, 10.1021/acs.jpca.6b10692, 2017.
533 Chu, Y., Sauerwein, M., and Chan, C. K.: Hygroscopic and phase transition properties
534 of alkyl aminium sulfates at low relative humidities, Physical chemistry chemical
535 physics : PCCP, 17, 19789-19796, 10.1039/c5cp02404h, 2015.
536 Clegg, S. L., Qiu, C., and Zhang, R.: The deliquescence behaviour, solubilities, and
537 densities of aqueous solutions of five methyl- and ethyl-aminium sulphate salts,
538 Atmospheric Environment, 73, 145-158, 10.1016/j.atmosenv.2013.02.036, 2013.
539 Ding, A., Nie, W., Huang, X., Chi, X., Sun, J., Kerminen, V.-M., Xu, Z., Guo, W.,
540 Petäjä, T., Yang, X., Kulmala, M., and Fu, C.: Long-term observation of air
541 pollution-weather/climate interactions at the SORPES station: a review and
542 outlook, Frontiers of Environmental Science & Engineering, 10,
543 10.1007/s11783-016-0877-3, 2016.
544 Ding, A. J., Fu, C. B., Yang, X. Q., Sun, J. N., Zheng, L. F., Xie, Y. N., Herrmann, E.,
545 Nie, W., Petäjä, T., Kerminen, V. M., and Kulmala, M.: Ozone and fine particle
546 in the western Yangtze River Delta: an overview of 1 yr data at the SORPES
547 station, Atmospheric Chemistry and Physics, 13, 5813-5830,
548 10.5194/acp-13-5813-2013, 2013a.

https://doi.org/10.5194/acp-2021-593
Preprint. Discussion started: 23 July 2021

549 Ding, A. J., Fu, C. B., Yang, X. Q., Sun, J. N., Petäjä, T., Kerminen, V. M., Wang, T.,
550 Xie, Y., Herrmann, E., Zheng, L. F., Nie, W., Liu, Q., Wei, X. L., and Kulmala,
551 M.: Intense atmospheric pollution modifies weather: a case of mixed biomass
552 burning with fossil fuel combustion pollution in eastern China, Atmospheric
553 Chemistry and Physics, 13, 10545-10554, 10.5194/acp-13-10545-2013, 2013b.
554 Facchini, M. C., Decesari, S., Rinaldi, M., Carbone, C., Finessi, E., Mircea, M., Fuzzi,
555 S., Moretti, F., Tagliavini, E., Ceburnis, D., and O'Dowd, C. D.: Important
556 source of marine secondary organic aerosol from biogenic amines,
557 Environmental science & technology, 42, 9116-9121, 10.1021/es8018385, 2008.
558 Ge, X., Wexler, A. S., and Clegg, S. L.: Atmospheric amines – Part I. A review,
559 Atmospheric Environment, 45, 524-546, 10.1016/j.atmosenv.2010.10.012,
560 2011a.
561 Ge, X., Wexler, A. S., and Clegg, S. L.: Atmospheric amines – Part II.
562 Thermodynamic properties and gas/particle partitioning, Atmospheric
563 Environment, 45, 561-577, 10.1016/j.atmosenv.2010.10.013, 2011b.
564 Healy, R. M., Evans, G. J., Murphy, M., Sierau, B., Arndt, J., McGillicuddy, E.,
565 O'Connor, I. P., Sodeau, J. R., and Wenger, J. C.: Single-particle speciation of
566 alkylamines in ambient aerosol at five European sites, Analytical and
567 bioanalytical chemistry, 407, 5899-5909, 10.1007/s00216-014-8092-1, 2015.
568 Huang, Y., Chen, H., Wang, L., Yang, X., and Chen, J.: Single particle analysis of
569 amines in ambient aerosol in Shanghai, Environmental Chemistry, 9, 202,
570 10.1071/en11145, 2012.
571 Huang, Y., Li, L., Li, J., Wang, X., Chen, H., Chen, J., Yang, X., Gross, D. S., Wang,
572 H., Qiao, L., and Chen, C.: A case study of the highly time-resolved evolution of
573 aerosol chemical and optical properties in urban Shanghai, China, Atmospheric
574 Chemistry and Physics, 13, 3931-3944, 10.5194/acp-13-3931-2013, 2013.
575 Lavi, A., Bluvshtein, N., Segre, E., Segev, L., Flores, M., and Rudich, Y.:
576 Thermochemical, Cloud Condensation Nucleation Ability, and Optical
577 Properties of Alkyl Aminium Sulfate Aerosols, The Journal of Physical
578 Chemistry C, 117, 22412-22421, 10.1021/jp403180s, 2013.
579 Li, L., Liu, L., Xu, L., Li, M., Li, X., Gao, W., Huang, Z., and Cheng, P.:
580 Improvement in the Mass Resolution of Single Particle Mass Spectrometry
581 Using Delayed Ion Extraction, Journal of the American Society for Mass
582 Spectrometry, 29, 2105-2109, 10.1007/s13361-018-2037-4, 2018.
583 Li, L., Huang, Z., Dong, J., Li, M., Gao, W., Nian, H., Fu, Z., Zhang, G., Bi, X.,
584 Cheng, P., and Zhou, Z.: Real time bipolar time-of-flight mass spectrometer for
585 analyzing single aerosol particles, International Journal of Mass Spectrometry,
586 303, 118-124, 10.1016/j.ijms.2011.01.017, 2011.
587 Lian, X., Zhang, G., Lin, Q., Liu, F., Peng, L., Yang, Y., Fu, Y., Jiang, F., Bi, X.,
588 Chen, D., Wang, X., Peng, P. a., and Sheng, G.: Seasonal variation of
589 amine-containing particles in urban Guangzhou, China, Atmospheric
590 Environment, 222, 117102, 10.1016/j.atmosenv.2019.117102, 2020.
591 Liu, Z., Chen, H., Li, Q., Sun, J., Wang, L., Yang, X., Xiao, H., Li, M., and Chen, J.:
592 Size‐Resolved Mixing States and Sources of Amine‐Containing Particles in

https://doi.org/10.5194/acp-2021-593
Preprint. Discussion started: 23 July 2021

593 the East China Sea, Journal of Geophysical Research: Atmospheres,
594 10.1029/2020jd033162, 2020.
595 Murphy, S. M., Sorooshian, A., Kroll, J. H., Ng, N. L., Chhabra, P., Tong, C., Surratt.,
596 J. D., Knipping, E., Flagan, R. C., and Seinfeld, J. H.: Secondary aerosol
597 formation from atmospheric reactions of aliphatic amines, Atmos. Chem. Phys, 7,
598 2313, 10.5194/ACP-7-2313-, 2007.
599 Nielsen, C. J., Bossi, R., Bunkan, A. J. C., Dithmer, L., Glasius, M., Hallquist, M.,
600 Hansen, A. M. K., Lutz, A., Salo, K., and Maguta, M. M.: Atmospheric
601 Degradation of Amines (ADA): summary report from atmospheric chemistry
602 studies of amines, nitrosamines, nitramines and amides, 2012.
603 Pitts, J. N., Grosjean, D., Van Cauwenberghe, K., Schmid, J. P., and Fitz, D. R.:
604 Photooxidation of aliphatic amines under simulated atmospheric conditions:
605 formation of nitrosamines, nitramines, amides, and photochemical oxidant,
606 Environmental science & technology, 12, 946-953, 10.1021/es60144a009, 1978.
607 Pratt, K. A., Hatch, L. E., and Prather, K. A.: Seasonal volatility dependence of
608 ambient particle phase amines, Environmental science & technology, 43,
609 5276-5281, 10.1021/es803189n, 2009.
610 Pratt, K. A., Murphy, S. M., Subramanian, R., DeMott, P. J., Kok, G. L., Campos, T.,
611 Rogers, D. C., Prenni, A. J., Heymsfield, A. J., Seinfeld, J. H., and Prather, K. A.:
612 Flight-based chemical characterization of biomass burning aerosols within two
613 prescribed burn smoke plumes, Atmospheric Chemistry and Physics, 11,
614 12549-12565, 10.5194/acp-11-12549-2011, 2011.
615 Price, D. J., Kacarab, M., Cocker, D. R., Purvis-Roberts, K. L., and Silva, P. J.:
616 Effects of temperature on the formation of secondary organic aerosol from amine
617 precursors, Aerosol Science and Technology, 50, 1216-1226,
618 10.1080/02786826.2016.1236182, 2016.
619 Price, D. J., Clark, C. H., Tang, X., Cocker, D. R., Purvis-Roberts, K. L., and Silva, P.
620 J.: Proposed chemical mechanisms leading to secondary organic aerosol in the
621 reactions of aliphatic amines with hydroxyl and nitrate radicals, Atmospheric
622 Environment, 96, 135-144, 10.1016/j.atmosenv.2014.07.035, 2014.
623 Qiu, C. and Zhang, R.: Physiochemical properties of alkylaminium sulfates:
624 hygroscopicity, thermostability, and density, Environmental science &
625 technology, 46, 4474-4480, 10.1021/es3004377, 2012.
626 Qiu, C., Wang, L., Lal, V., Khalizov, A. F., and Zhang, R.: Heterogeneous reactions
627 of alkylamines with ammonium sulfate and ammonium bisulfate, Environmental
628 science & technology, 45, 4748-4755, 10.1021/es1043112, 2011.
629 Rehbein, P. J., Jeong, C. H., McGuire, M. L., Yao, X., Corbin, J. C., and Evans, G. J.:
630 Cloud and fog processing enhanced gas-to-particle partitioning of
631 trimethylamine, Environmental science & technology, 45, 4346-4352,
632 10.1021/es1042113, 2011.
633 Rovelli, G., Miles, R. E. H., Reid, J. P., and Clegg, S. L.: Hygroscopic properties of
634 aminium sulfate aerosols, Atmospheric Chemistry and Physics, 17, 4369-4385,
635 10.5194/acp-17-4369-2017, 2017.

https://doi.org/10.5194/acp-2021-593
Preprint. Discussion started: 23 July 2021

636 Sauerwein, M. and Chan, C. K.: Heterogeneous uptake of ammonia and
637 dimethylamine into sulfuric and oxalic acid particles, Atmospheric Chemistry
638 and Physics, 17, 6323-6339, 10.5194/acp-17-6323-2017, 2017.
639 Silva, P. J., Erupe, M. E., Price, D., Elias, J., Malloy, Q. G., Li, Q., Warren, B., and
640 Cocker, D. R., 3rd: Trimethylamine as precursor to secondary organic aerosol
641 formation via nitrate radical reaction in the atmosphere, Environmental science
642 & technology, 42, 4689-4696, 10.1021/es703016v, 2008.
643 Sorooshian, A., Murphy, S., Hersey, S., Gates, H., Padro, L., Nenes, A., Brechtel, F.,
644 Jonsson, H., Flagan, R., and Seinfeld, J.: Comprehensive airborne
645 characterization of aerosol from a major bovine source, Atmospheric Chemistry
646 and Physics, 8, 5489-5520, 2008.
647 Tang, X., Price, D., Praske, E., Lee, S. A., Shattuck, M. A., Purvis-Roberts, K., Silva,
648 P. J., Asa-Awuku, A., and Cocker, D. R.: NO3 radical, OH radical and
649 O3-initiated secondary aerosol formation from aliphatic amines, Atmospheric
650 Environment, 72, 105-112, 10.1016/j.atmosenv.2013.02.024, 2013.
651 Tao, Y., Ye, X., Jiang, S., Yang, X., Chen, J., Xie, Y., and Wang, R.: Effects of
652 amines on particle growth observed in new particle formation events, Journal of
653 Geophysical Research: Atmospheres, 121, 324-335, 10.1002/2015jd024245,
654 2016.
655 Tong, D., Chen, J., Qin, D., Ji, Y., Li, G., and An, T.: Mechanism of atmospheric
656 organic amines reacted with ozone and implications for the formation of
657 secondary organic aerosols, The Science of the total environment, 737, 139830,
658 10.1016/j.scitotenv.2020.139830, 2020.
659 Tuazon, E. C., Martin, P., Aschmann, S. M., Arey, J., and Atkinson, R.: Kinetics of
660 the reactions of OH radicals with 2-methoxy-6-(trifluoromethyl)pyridine,
661 diethylamine, and 1,1,3,3,3-pentamethyldisiloxan-1-ol at 298 ± 2 K,
662 International Journal of Chemical Kinetics, 43, 631-638, 10.1002/kin.20594,
663 2011.
664 Wang, L., Lal, V., Khalizov, A. F., and Zhang, R.: Heterogeneous chemistry of
665 alkylamines with sulfuric acid: Implications for atmospheric formation of
666 alkylaminium sulfates, Environmental science & technology, 44, 2461-2465,
667 2010.
668 Yin, S., Ge, M., Wang, W., Liu, Z., and Wang, D.: Uptake of gas-phase alkylamines
669 by sulfuric acid, Chinese Science Bulletin, 56, 1241-1245,
670 10.1007/s11434-010-4331-9, 2011.
671 Youn, J. S., Crosbie, E., Maudlin, L. C., Wang, Z., and Sorooshian, A.:
672 Dimethylamine as a major alkyl amine species in particles and cloud water:
673 Observations in semi-arid and coastal regions, Atmos Environ (1994), 122,
674 250-258, 10.1016/j.atmosenv.2015.09.061, 2015.
675 Zhang, G., Bi, X., Chan, L. Y., Li, L., Wang, X., Feng, J., Sheng, G., Fu, J., Li, M.,
676 and Zhou, Z.: Enhanced trimethylamine-containing particles during fog events
677 detected by single particle aerosol mass spectrometry in urban Guangzhou,
678 China, Atmospheric Environment, 55, 121-126, 10.1016/j.atmosenv.2012.03.038,
679 2012.

https://doi.org/10.5194/acp-2021-593
Preprint. Discussion started: 23 July 2021

680 Zhang, G., Lian, X., Fu, Y., Lin, Q., Li, L., Song, W., Wang, Z., Tang, M., Chen, D.,
681 Bi, X., Wang, X., and Sheng, G.: High secondary formation of
682 nitrogen-containing organics (NOCs) and its possible link to oxidized organics
683 and ammonium, Atmospheric Chemistry and Physics, 20, 1469-1481,
684 10.5194/acp-20-1469-2020, 2020.
685 Zhang, J., Luo, B., Zhang, W., Rao, Z., and Song, H.: Single-particle characterization
686 of amine-containing particles during summer and winter in Chengdu, CHINA
687 ENVIRONMENTAL SCIENCECE, 39, 3152-3160, 2019.
688 Zhao, J., Smith, J. N., Eisele, F. L., Chen, M., Kuang, C., and McMurry, P. H.:
689 Observation of neutral sulfuric acid-amine containing clusters in laboratory and
690 ambient measurements, Atmospheric Chemistry and Physics, 11, 10823-10836,
691 10.5194/acp-11-10823-2011, 2011.
692 Zhou, S., Li, H., Yang, T., Chen, Y., Deng, C., Gao, Y., Chen, C., and Xu, J.:
693 Characteristics and sources of aerosol aminiums over the eastern coast of China:
694 insights from the integrated observations in a coastal city, adjacent island and
695 surrounding marginal seas, Atmospheric Chemistry and Physics, 19,
696 10447-10467, 10.5194/acp-19-10447-2019, 2019.
697

https://doi.org/10.5194/acp-2021-593
Preprint. Discussion started: 23 July 2021

Atmospheric Chemistry and Physics Discussions

Tables and figures

Table list:

Table 1. Summary of the major species of detected amine-containing particles and fragments in September in Nanjing, China.

Table 2. The linear correlations (r^2) between secondary ion-containing amine particles within TMA- and DEA-containing particles.

Table 3. Number fractions sulfate, nitrate, and ammonium in TMA-containing particles, DEA-containing particles, and total particles.

Figure caption:

Figure 1. Temporal variations in relative humidity (RH), temperature (T), O_3 concentration, $PM_{2.5}$ concentration, wind speed, wind direction, and TMA- and DEA-containing particles during the entire sampling period.

Figure 2. Backward trajectories (48 h) of air masses at 500 m above the ground during the sampling period: (a) TMA-containing particles counts; (b) DEA-containing particle counts. C1 to C4 represent cluster 1 to cluster 4.

Figure 3. The diurnal variations in particle counts and number fractions of the two amine-containing particles in total particles during the entire sampling period.

Figure 4. Particle counts of amine-containing particles and relative peak area (RPA) of the two amines in single particles, with an increase in ambient RH. (a, c) TMA-containing particles; (b, d) DEA-containing particles.

Figure 5. Mass spectra of TMA- and DEA-containing particles during the entire sampling period.

Figure 6. Differential mass spectra between DEA- and TMA-containing particles.

Figure 7. (a) Temporal trends of the relative peak areas (RPAs) of $^{73}C_3H_5O_2^-$, $^{89}HC_2O_4^-$, $^{26}CN^-$, and $^{42}CNO^-$ in DEA-containing particles. **(b)** Diurnal variations in the relative RPAs of $^{73}C_3H_5O_2^-$, $^{89}HC_2O_4^-$, $^{26}CN^-$, and $^{42}CNO^-$ in DEA-containing particles.

https://doi.org/10.5194/acp-2021-593
Preprint. Discussion started: 23 July 2021

Atmospheric Chemistry and Physics Discussions

727 **Figure 8.** Differential mass spectra of DEA-containing particles between 22:00–02:00
728 and 14:00–18:00.
729 **Figure 9.** Temporal trends of RPA nitrate in DEA-containing particles, number
730 fraction of DEA-containing particles in total particles, and NOx concentration.
731 **Figure 10.** Temporal trends of TMA- and DEA-containing particle counts, and
732 number fractions of nitrate, sulfate, and ammonium in TMA- and DEA-containing
733 particles.
734 **Figure 11.** Temporal trends of the relative acidity ratios (Ra, Ra') in TMA- and
735 DEA-containing particles.
736
737
738
739
740
741
742
743
744
745
746
747
748
749
750
751
752
753
754
755
756
757
758
759
760
761
762
763
764
765

https://doi.org/10.5194/acp-2021-593
Preprint. Discussion started: 23 July 2021

Atmospheric Chemistry and Physics Discussions

766 ## Tables

767 **Table 1.** Summary of the major species of detected amine-containing particles and
768 fragments in September in Nanjing, China.

Alkylamine assignment	Count	Percentage (%)
All detected particles	4 693 931	
$^{59}(CH_3)_3N^+$ (TMA)-containing particles	1072143	22.8
$^{74}(C_2H_5)_2NH_2^+$ (DEA) -containing particles	259913	5.5
$^{86}(C_2H_5)_2NCH_2^+$ (TEA)-containing particles	172621	3.7

769
770
771

772 **Table 2.** The linear correlations (r^2) between secondary ion-containing amine
773 particles within TMA- and DEA-containing particles.

	TMA particles	DEA particles
$^{26}CN^-$	0.13	0.70
$^{42}CNO^-$	0.09	0.70
$^{73}C_3H_5O_2^-$	0.01	0.66
$^{89}HC_2O_4^-$	0.09	0.57
$^{43}C_2H_3O^+$	0.05	0.90
$^{62}NO_3^-$	0.93	0.90
$^{97}HSO_4^-$	0.32	0.86
$^{18}NH_4^+$	0.50	0.28

774
775
776
777

778 **Table 3.** Number fractions sulfate, nitrate, and ammonium in TMA-containing
779 particles, DEA-containing particles, and total particles.

	TMA particles	DEA particles	Total particles
Sulfate	55.3	79.3	60.1
Nitrate	81.6	81.8	72.0
Ammonium	35.0	13.2	19.4

780
781
782
783

https://doi.org/10.5194/acp-2021-593
Preprint. Discussion started: 23 July 2021

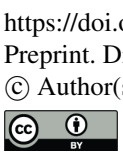

Atmospheric Chemistry and Physics Discussions

784 **Figures**

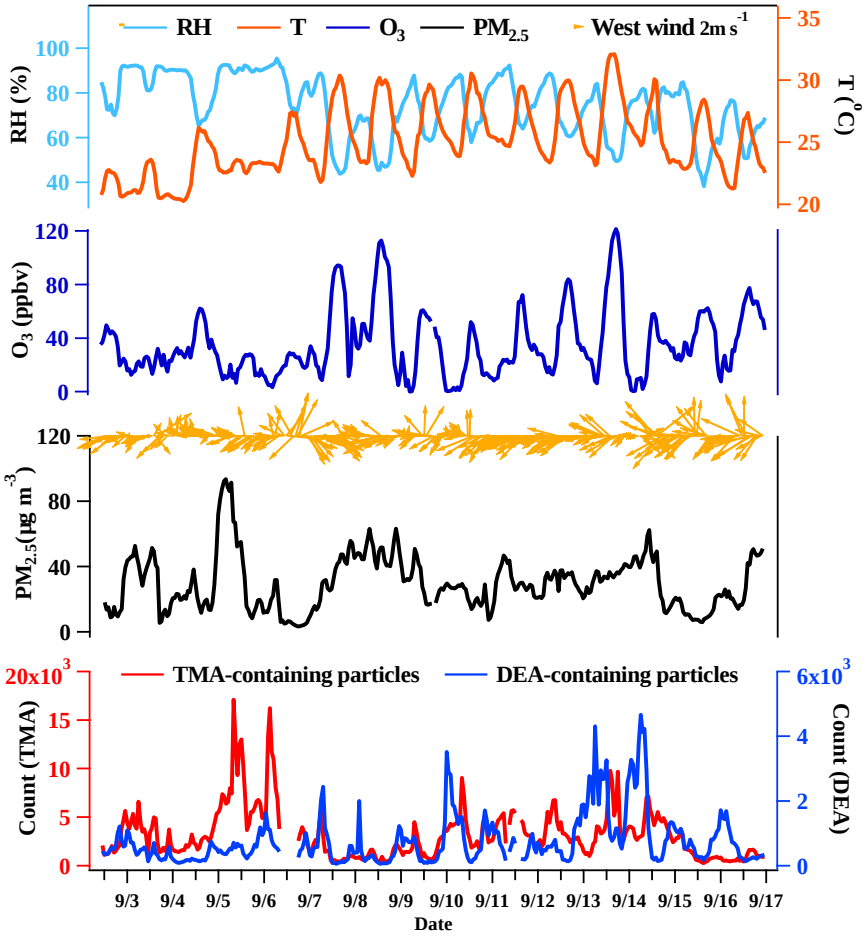

785

786 **Figure 1.** Temporal variations in relative humidity (RH), temperature (T), O_3
787 concentration, $PM_{2.5}$ concentration, wind speed, wind direction, and TMA- and
788 DEA-containing particles during the entire sampling period.

789

790

791

792

793

794

https://doi.org/10.5194/acp-2021-593
Preprint. Discussion started: 23 July 2021

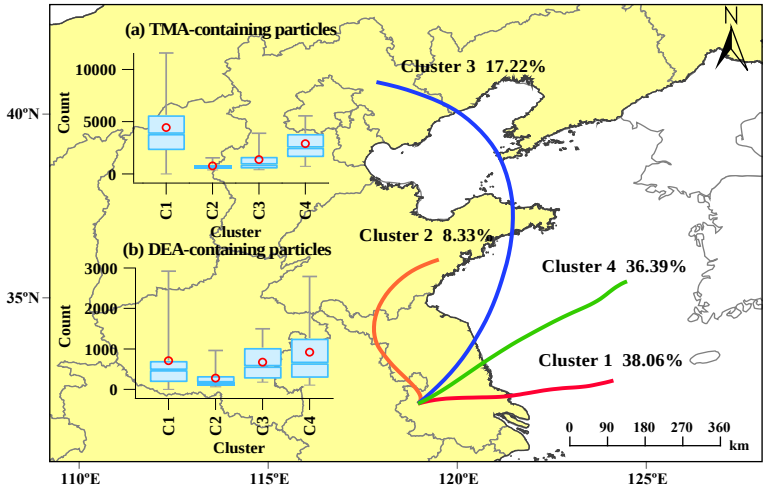

Figure 2. Backward trajectories (48 h) of air masses at 500 m above the ground during the sampling period: (a) TMA-containing particles counts; (b) DEA-containing particle counts. C1 to C4 represent cluster 1 to cluster 4.

https://doi.org/10.5194/acp-2021-593
Preprint. Discussion started: 23 July 2021

Atmospheric Chemistry and Physics Discussions

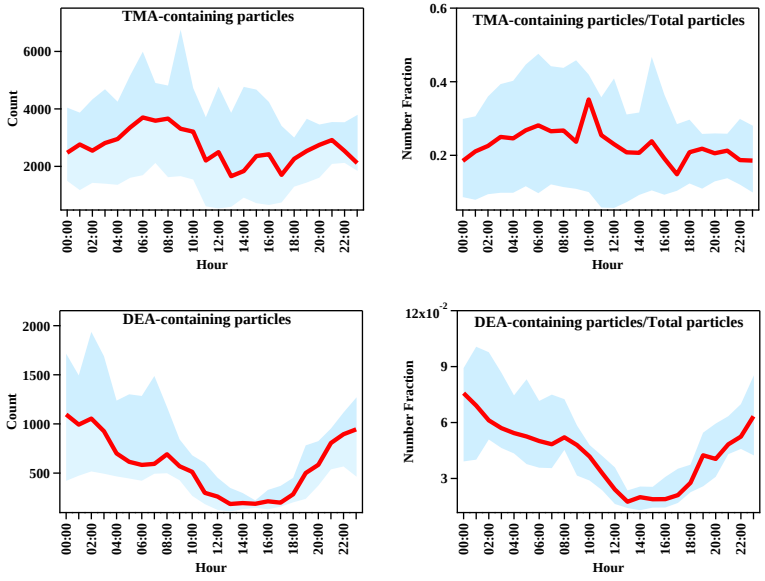

Figure 3. The diurnal variations in particle counts and number fractions of the two amine-containing particles in total particles during the entire sampling period. The shaded areas represent the 75th and 25th percentiles.

https://doi.org/10.5194/acp-2021-593
Preprint. Discussion started: 23 July 2021

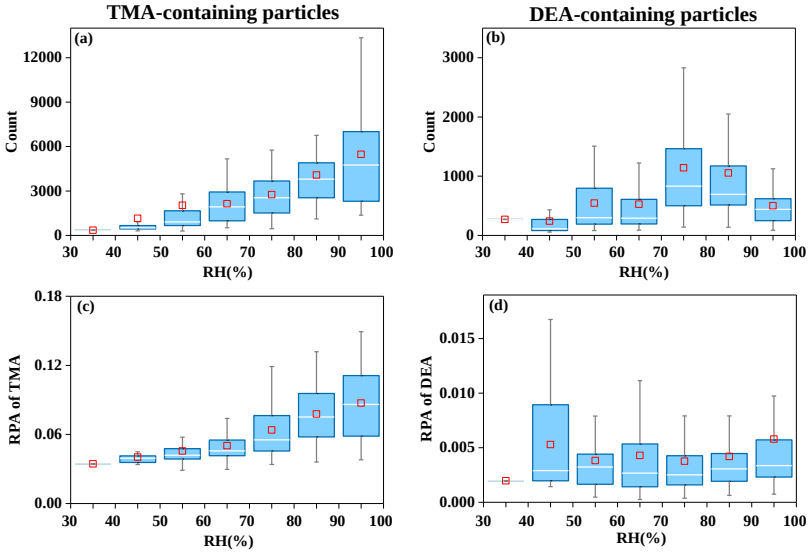

Figure 4. Particle counts of amine-containing particles and relative peak area (RPA) of the two amines in single particles, with an increase in ambient RH. (a, c) TMA-containing particles; (b, d) DEA-containing particles. Squares represent the average values. The line inside the box indicates the median. Upper and lower boundaries of the box represent the 75th and the 25th percentiles; the whiskers above and below each box represent the 95th and 5th percentiles.

https://doi.org/10.5194/acp-2021-593
Preprint. Discussion started: 23 July 2021

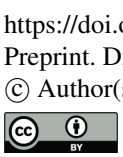

Atmospheric Chemistry and Physics Discussions

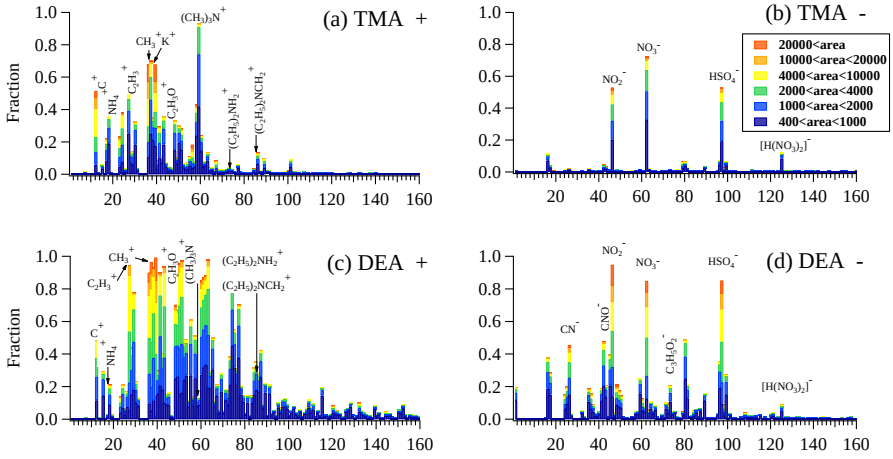

Figure 5. Mass spectra of TMA- and DEA-containing particles during the entire sampling period.

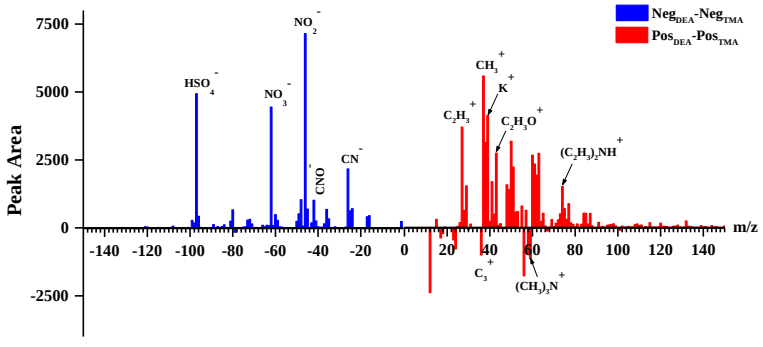

Figure 6. Differential mass spectra between DEA- and TMA-containing particles.

https://doi.org/10.5194/acp-2021-593
Preprint. Discussion started: 23 July 2021

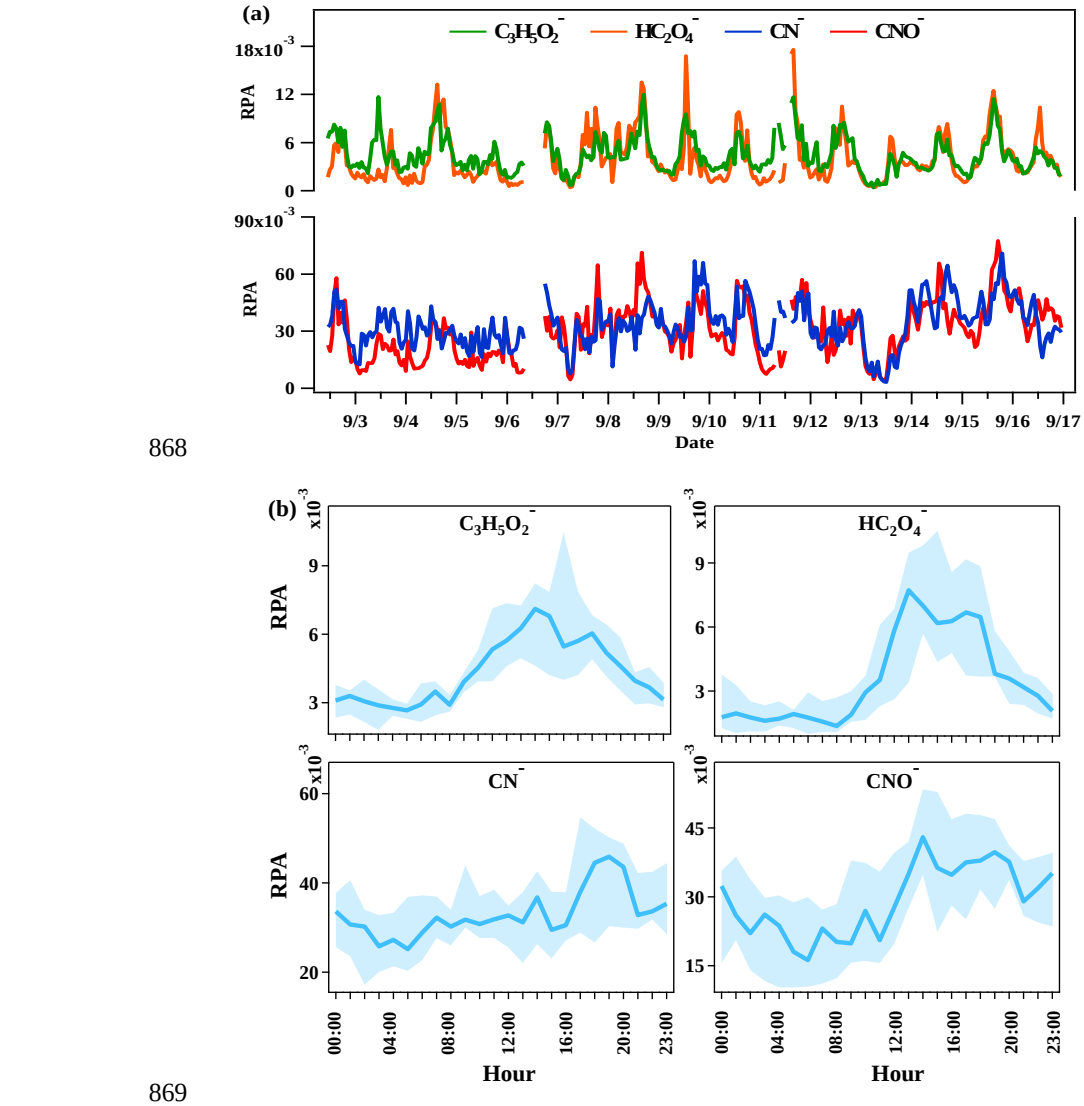

Figure 7. (a) Temporal trends of the relative peak areas (RPAs) of $^{73}C_3H_5O_2^-$, $^{89}HC_2O_4^-$, $^{26}CN^-$, and $^{42}CNO^-$ in DEA-containing particles. **(b)** Diurnal variations in the relative RPAs of $^{73}C_3H_5O_2^-$, $^{89}HC_2O_4^-$, $^{26}CN^-$, and $^{42}CNO^-$ in DEA-containing particles. The shaded areas represent the 75th and 25th percentiles.

https://doi.org/10.5194/acp-2021-593
Preprint. Discussion started: 23 July 2021

Atmospheric Chemistry and Physics Discussions

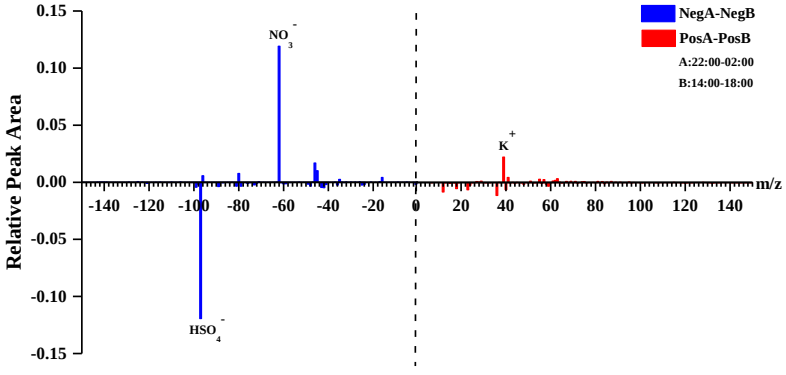

877

878 **Figure 8.** Differential mass spectra of DEA-containing particles between 22:00–02:00

879 and 14:00–18:00.

880

881

882

883

884

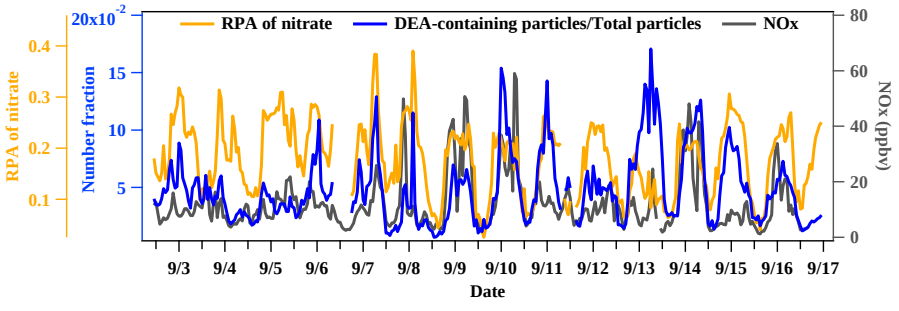

885

886 **Figure 9.** Temporal trends of RPA nitrate in DEA-containing particles, number

887 fraction of DEA-containing particles in total particles, and NOx concentration.

888

889

890

891

892

https://doi.org/10.5194/acp-2021-593
Preprint. Discussion started: 23 July 2021

Atmospheric Chemistry and Physics Discussions

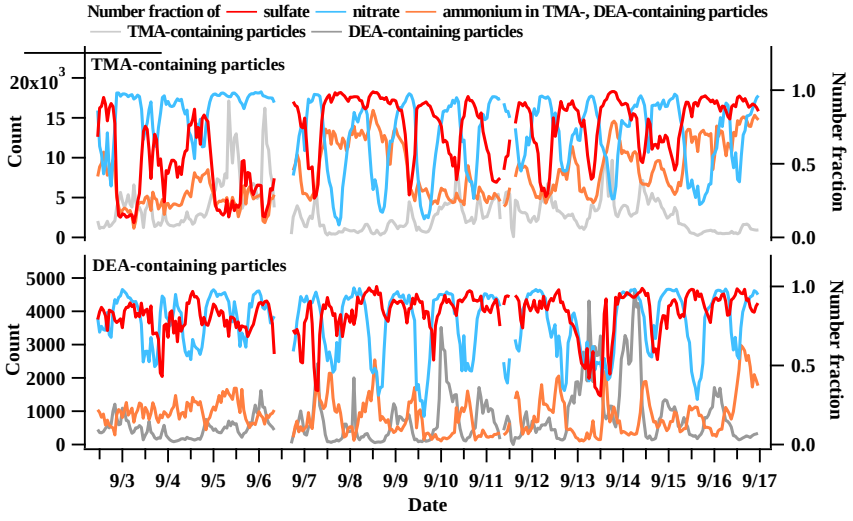

Figure 10. Temporal trends of TMA- and DEA-containing particle counts, and number fractions of nitrate, sulfate, and ammonium in TMA- and DEA-containing particles.

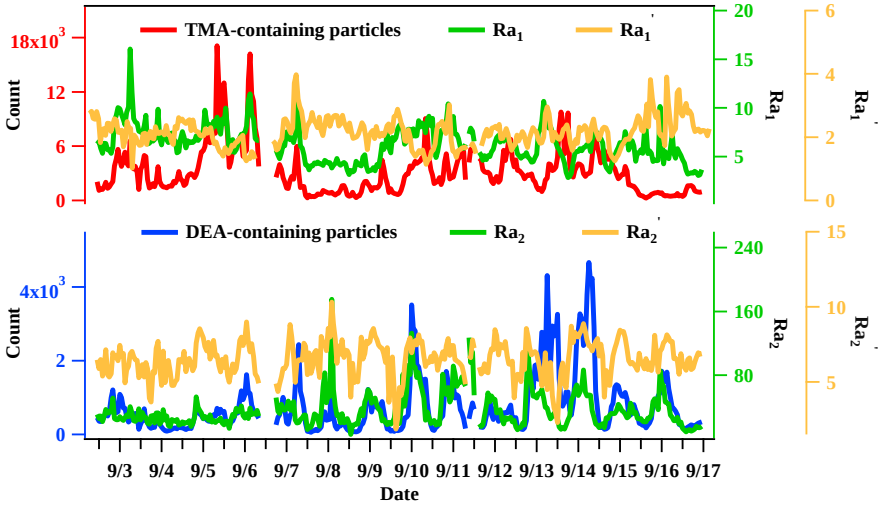

Figure 11. Temporal trends of the relative acidity ratios (Ra, Ra') in TMA- and DEA-containing particles.